



# International Journal of Research in Agronomy

E-ISSN: 2618-0618  
P-ISSN: 2618-060X  
© Agronomy  
NAAS Rating (2025): 5.20  
[www.agronomyjournals.com](http://www.agronomyjournals.com)  
2025; SP-8(9): 31-45  
Received: 25-06-2025  
Accepted: 27-07-2025

**Ananya Mishra**  
Ph.D., Research Scholar,  
Department of Soil and Water  
Conservation Engineering, College  
of Agricultural Engineering &  
Technology, JAU, Junagadh,  
Gujarat, India

**HD Rank**  
Head of Department, Department  
of Soil and Water Conservation  
Engineering, College of  
Agricultural Engineering &  
Technology, JAU, Junagadh,  
Gujarat, India

**Corresponding Author:**  
**Ananya Mishra**  
Ph.D., Research Scholar,  
Department of Soil and Water  
Conservation Engineering, College  
of Agricultural Engineering &  
Technology, JAU, Junagadh,  
Gujarat, India

## Evaluating temperature bias corrections in regional climate models: Insights from Rajkot's historical and future data

**Ananya Mishra and HD Rank**

**DOI:** <https://www.doi.org/10.33545/2618060X.2025.v8.i9Sa.3712>

### Abstract

This study evaluates bias correction of the Regional Climate Model (RCM) outputs from the CORDEX South Asia dataset for Rajkot district of Gujarat, using data from the Indian Meteorological Department (IMD). It focused mainly on daily maximum and minimum temperatures during the historical period (1951-2005) and future projections (2006-2100) under RCP 2.6, RCP 4.5, and RCP 8.5. The bias correction method used was Gaussian distribution mapping, and statistical parameters such as monthly mean, coefficient of variation (CV), skewness (Cs), and kurtosis (Ck) were analysed. During the control period (1951-2005), raw RCM data was found underestimated than the observed IMD temperature data. After bias correction, monthly means closely matched the observations, with an  $R^2$  of 1.00 for both maximum and minimum temperatures during calibration (1951-1995) and validation (1996-2005). The CV improved significantly after correction, with values aligning with IMD. However, the Gaussian method failed to correct higher-order moments such as skewness (Cs) remained negative during calibration but became positive for some months during validation, and kurtosis (Ck) stayed positive for all months, indicating the persistence of heavy-tailed distributions. For future scenarios (2006-2100), bias-corrected RCM data was found overestimated for monthly mean temperatures across all RCPs. The CV was consistently lower than in raw data. Skewness (Cs) and kurtosis (Ck) showed varied results: under RCP 2.6 and RCP 4.5, Cs was mostly positive in winter months, while Ck was positive in both summer and winter. Under RCP 8.5, skewness and kurtosis were positive for most months. Overall, Gaussian distribution mapping effectively corrected the mean temperature values and provided a solid foundation for temperature projections, making it a valuable method for adjusting climate models, though further refinement may be needed to address the extreme temperature events for enhanced climate resilience planning.

**Keywords:** IMD, CORDEX, bias correction, RCM, Gaussian distribution, temperature projections, RCP, climate adaptation, Rajkot, Gujarat

### Introduction

Global and regional climate models (GCMs and RCMs) frequently exhibit biases, which necessitate correction against observational or reanalysis datasets to ensure their outputs are suitable for impact studies and practical applications, such as evaluating the effects of climate change on climate extremes (Eccles *et al.*, 2021; Trancoso *et al.*, 2020) [3, 9]. GCMs simulate atmospheric circulation patterns but with a coarse spatial resolution of 100-200 km. Compared to GCMs, RCMs are more adept at capturing mesoscale precipitation patterns, including topographic effects and sea-land contrasts (Frei *et al.*, 2006; Grose *et al.*, 2019) [5, 6]. However, RCMs still exhibit significant biases due to factors such as imperfect boundary conditions derived from reanalysis or GCM data and systematic errors inherent in the model itself (Ehret *et al.*, 2012; Teutschbein & Seibert, 2012) [4, 8].

Bias correction is a crucial preliminary step in most climate change impact studies and involves adjusting model outputs to reduce systematic errors, thereby improving their fit to observed data (Maraun, 2016) [7]. There are various methods of bias correction, ranging from simple linear scaling to more sophisticated techniques like quantile mapping (Casaneuva *et al.*, 2020; Chen *et al.*, 2013) [1, 2]. Linear scaling adjusts projections by accounting for monthly errors but only corrects the mean, which can be inadequate for extreme events and other statistical characteristics, such as variability (Teutschbein and Seibert, 2012) [8].

In contrast, distribution mapping methods, including quantile-quantile mapping, can correct for both variability and extremes, offering a more comprehensive approach to bias correction (Teutschbein and Seibert, 2012)<sup>[8]</sup>.

The Coordinated Regional Downscaling Experiment (CORDEX) provides enhanced regional climate change projections on a global scale, offering detailed predictions that can be easily applied to any region. These datasets are valuable for vulnerability and adaptation studies as well as climate research. In the past, climate change impact assessments primarily relied on General Circulation Models (GCMs) or Regional Climate Models (RCMs), but CORDEX has expanded the ability to produce more refined and region-specific climate projections.

CORDEX data, like other climate model outputs, often exhibit biases that necessitate careful analysis when studying future climate projections. To address these biases, it is essential to compare future simulations (post-2006) with historical simulations (1961-2005) produced by the same CORDEX models. This comparison helps in understanding the deviations and provides a more accurate representation of future climate conditions. The CORDEX initiative offers data for three key Representative Concentration Pathways (RCPs) - RCP 2.6, RCP 4.5 and RCP 8.5 - which represent different possible scenarios for greenhouse gas emissions and land-use changes. By examining these scenarios, researchers can better understand the potential range of future climate outcomes and their implications.

RCP 8.5 represents the most pessimistic scenario, where no significant climate policy is implemented, leading to high population growth and elevated levels of greenhouse gas emissions by 2100. This scenario assumes a future where the global community fails to take substantial action to mitigate climate change, resulting in severe environmental consequences. On the other hand, RCP 4.5 depicts a more moderate scenario, where efforts are made to stabilize greenhouse gas emissions by the end of the century. This pathway suggests that, while some measures are taken to address climate change, they are not aggressive enough to reverse the trends entirely, leading to a stabilized but warmer climate. RCP 2.6 is the most optimistic scenario, assuming a significant reduction in greenhouse gas emissions, resulting in a projected global temperature rise of only 1.6°C by 2100 relative to pre-industrial levels. This scenario envisions a future where strong international cooperation and stringent climate policies lead to substantial mitigation efforts, keeping global warming to a minimum. Comparing climate projections across these three scenarios is crucial for understanding the potential impacts of varying levels

of anthropogenic activity, particularly in terms of greenhouse gas emissions. The differences between these pathways highlight the importance of policy decisions and their long-term effects on the global climate.

In recent years, the increasing frequency of extreme climate events has underscored the need to analyze future climate projections using Regional Climate Models (RCMs) under different RCP scenarios. These extreme events, ranging from heatwaves to intense storms, are becoming more common as the climate continues to change, posing significant challenges for communities and ecosystems worldwide. However, the outputs of RCMs, like all climate models, are not free from biases. These biases must be corrected to ensure that the projections are accurate and reliable, especially when used for decision-making in climate adaptation and mitigation efforts.

This study aims to assess the effectiveness of distribution mapping techniques for bias correction in temperature data simulated by the RCA4 RCM for a specific study area under different RCP scenarios. By focusing on bias correction, the study seeks to improve the reliability of climate projections, providing more accurate data for researchers and policymakers. This approach is critical for developing effective strategies to address the impacts of climate change, particularly in regions that are highly vulnerable to shifts in temperature and precipitation patterns.

### Study Area

Rajkot is a prominent city located in the Saurashtra region of Gujarat, India, and serves as the administrative headquarters of the Rajkot district. It is situated at 22.3039°N latitude and 70.8022°E longitude. Rajkot ranks as the fourth-largest city in Gujarat in terms of population. Rajkot is positioned in the central part of the Saurashtra peninsula, on the banks of the Aji and Nyari rivers. Rajkot experiences a semi-arid climate, characterized by three main seasons. Summer (March to June): Summers in Rajkot are hot, with temperatures often ranging from 24 °C to 42 °C. The peak of summer usually sees maximum temperatures around 40 °C, accompanied by dry and sunny weather. Monsoon (July to September): The city receives the majority of its annual rainfall during the monsoon season, with July and August being the wettest months. The average annual rainfall is approximately 500-600 mm. The monsoon season brings relief from the intense heat, but high humidity levels are typical. Winter (October to February): Winters in Rajkot are mild, with temperatures ranging between 10 °C and 25 °C. The season is generally dry, and the weather remains pleasant.



**Fig 1:** Study area map showing Rajkot District

## Data Collection

The research utilized gridded rainfall and temperature data prepared by the Indian Meteorological Department (IMD) for various regions in India. The datasets included daily gridded rainfall at a 0.25 x 0.25-degree resolution and daily maximum and minimum temperatures at a 0.5 x 0.5-degree resolution. These datasets were provided in the Network Common Data Format (NetCDF). To access and process this data, the NetCDF4Excel add-in can be downloaded and installed, enabling the conversion of NetCDF files to Excel format using ArcGIS software.

This climatic data was crucial for studying future climate change projections. Regional Climate Models (RCMs) are effective tools for understanding and predicting climate changes. In this research, climate change data was sourced from the CORDEX-South Asia Multi-Model Output, accessible through the Centre for Climate Change Research at the Indian Institute of Tropical Meteorology, Pune. The CORDEX data includes simulations using the RCA4 (Rossby Centre regional atmospheric model version 4) model for various regions, available at two resolutions: the standard 0.44 degrees (~50 km, EUR-44) and a finer 0.11 degrees (~12.5 km, EUR-11). These datasets provide projections for daily rainfall (in mm) and temperature (in °C) under different Representative Concentration Pathway (RCP) scenarios—2.6, 4.5, and 8.5—covering both historical and future periods. Similar to the IMD data, these climate data file, also in NetCDF format, were converted to Excel format using ArcGIS for further analysis.

## Methodology

The historical daily maximum and minimum temperature records for Junagadh, covering 55 years (1951-2005), were obtained from the Indian Meteorological Department (IMD). Simulated maximum and minimum temperatures for the same location were also acquired from the CORDEX database for various Representative Concentration Pathways (RCPs). The baseline period (1951-2005) was used as a reference for comparison with future projections (2006-2100) under different RCP scenarios, including RCP 2.6, RCP 4.5, and RCP 8.5.

Simulations from Regional Climate Models (RCMs) often exhibit biases due to inherent model errors, such as inaccuracies in model formulation, spatial discretization, and grid cell averaging. These biases make direct application of RCM outputs in hydrological impact studies challenging. To address this, it is recommended to use an ensemble of RCM simulations and apply bias correction techniques. These methods adjust the simulated climate data to better match observed values. In this study, the period from 1951 to 1995 was used for model calibration, while 1996 to 2005 served as the validation period. A probability distribution-based scaling method was applied to correct the RCM-simulated temperatures. This method uses cumulative distribution functions to align the simulated data with observed temperature distributions. The annual temperature cycle, being symmetric, was modeled using a normal distribution with monthly-specific means and standard deviations, allowing for a more accurate representation of temperature variability.

## Distribution Mapping Method

The Distribution Mapping (DM) method was used to align the

distribution of modeled data with that of observed data. This method adjusts key statistical parameters, such as the mean, standard deviation, and quantiles, while aiming to maintain the integrity of extreme values. However, a limitation of this approach in the assumption that both observed and simulated meteorological variables share the same underlying distribution, which may not always be the case and can introduce additional biases.

For temperature time series, the Gaussian distribution method was often assumed to be the most suitable. This distribution defined by two parameters: the mean ( $\mu$ ), which determines the centre of the distribution, and the standard deviation ( $\sigma$ ), which influences its spread. A smaller standard deviation ( $\sigma$ ) results in a narrower distribution with fewer extreme values, while a larger standard deviation leads to a wider distribution, increasing the probability of extremes. To adjust the temperature data using this method, the Gaussian cumulative distribution function (CDF) and its inverse are applied, allowing for the transformation of simulated data to more closely resemble observed data.

For temperature adjustments, the process involves using the Gaussian (normal) CDF ( $F_N$ ) cumulative distribution function (CDF) and its inverse ( $F_N^{-1}$ ).

$$T_{contr}^* = F_N^{-1}(F_N(T_{contr}(d) | \mu_{contr,m}, \sigma_{contr,m}^2) | \mu_{obs,m}, \sigma_{obs,m}^2) \quad (1)$$

$$T_{scen}^* = F_N^{-1}(F_N(T_{scen}(d) | \mu_{contr,m}, \sigma_{contr,m}^2) | \mu_{obs,m}, \sigma_{obs,m}^2) \quad (2)$$

Where,

- $T_{contr}^*$  = corrected value of temperature of control period
- $T_{contr}$  = uncorrected value of temperature of control period
- $T_{scen}^*$  = corrected value of temperature for scenario period
- $T_{scen}$  = uncorrected value of temperature of scenario period
- $F_N$  = Gaussian CDF
- $F_N^{-1}$  = Inverse Gaussian CDF
- $\mu_{contr}$  = monthly mean of simulated time series of daily temperature during for control period
- $\sigma_{obs}^2$  = monthly standard deviation of observed time series of temperature during control period
- $\mu_{obs}$  = monthly mean of observed time series of daily temperature during control period
- $\sigma_{contr}^2$  = monthly standard deviation of simulated time series of daily temperature during control period.

## Results and Discussion

The study focused on bias corrections for daily maximum and minimum temperatures, covering both a baseline period (1951-2005) and future scenarios (2006-2100). It involved calibration (1951-1995) and validation (1996-2005) phases, comparing simulated data with actual observations. Specifically, the bias correction was applied to temperatures simulated by RCA4 for Rajkot, using observed data for comparison. The analysis provided temperature data for both the control period (1951-2005) and the projected future period (2006-2100).

### A) Daily Maximum Temperature Control Period (1951-2005)

The computed monthly mean of daily observed, Raw RCM and Bias corrected RCM of maximum temperature of Rajkot for the



calibration period (1951-1995) and validation period of (1996-2005) shown in Fig 1a.1 and Fig 1a.2. The considered statistics were the mean and coefficient of variation of the bias correction using the gaussian distribution mapping method. Fig 1a.1 showed that the raw RCM maximum temperature was underestimated over the observed monthly maximum temperature for all months for calibration period and Fig 1a.2 also showed the same result for the validation period. In fact, after applying the bias correction of Gaussian distribution method, the monthly mean for calibration period, (Fig 1a.1) and monthly mean for the validation period, (Fig 1a.2) of daily maximum temperature were agreed well with the actual observation during all of the 12 months of the year.

The relationship of monthly mean of observed maximum, raw RCM and bias corrected RCM maximum temperature for calibration period (1951-1995) and validation period (1996-2005) were shown in Fig 1a.3 and Fig 1a.4. It could be seen from Fig 1a.3 that goodness of fit ( $R^2$ ) between raw RCM and Bias corrected RCM were 0.91 and 1 respectively for calibration period (1951-1995) and Fig 1a.4 showed that goodness of fit ( $R^2$ ) between raw RCM and Bias corrected RCM were 0.921 and 0.999 respectively for validation period (1996-2005), which showed that the gaussian distribution has corrected the first moment.

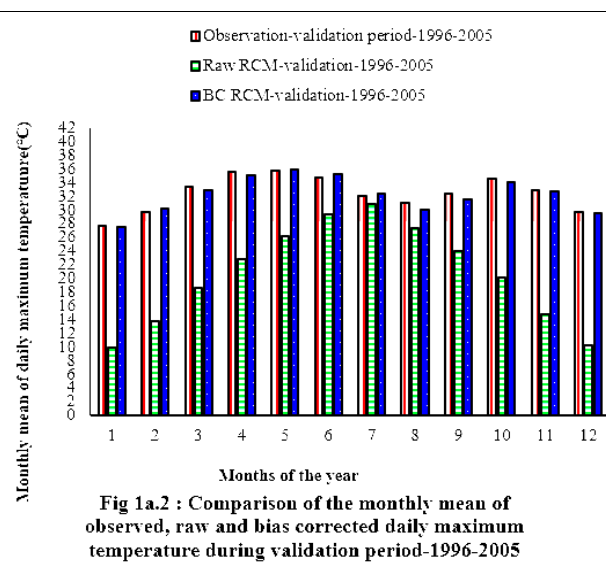
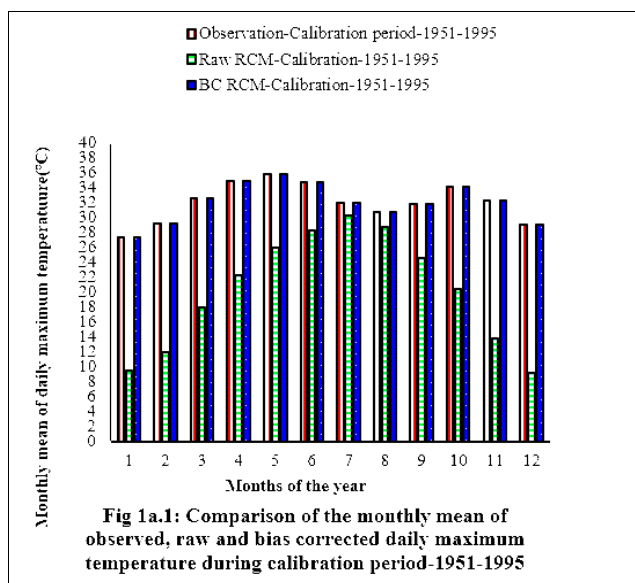
The coefficient of variation of observed, raw RCM and Bias corrected RCM daily maximum temperature of Rajkot during the calibration and validation period was found as shown in Fig 1a.5 and Fig 1a.6. Fig 1a.5 Showed that the raw RCM daily maximum temperature with higher coefficient of variation than the observed maximum temperature data for all months. After applying the bias correction, the coefficient of variation of BC RCM maximum temperature were matched with the observed coefficient of variation of maximum temperature. For validation

period (1996-2005), the coefficient of variation of both observed and bias corrected data were found lower than the coefficient of variation of raw RCM maximum temperature for all months. However, after applying the bias correction, the coefficient of variation of BC RCM maximum temperature were matched with the observed coefficient of variation of maximum temperature.

The relationship between the monthly coefficient of variation of observed, Raw and bias corrected daily maximum temperature for calibration period (1951-1995) and validation period (1996-2005) were shown in Fig 1a.7 and Fig 1a.8. It could be seen from Fig 1a.7 that goodness of fit ( $R^2$ ) between raw RCM and Bias corrected RCM were 0.883 and 1 respectively for calibration period (1951-1995) which shows that data set was nearly matched with each other and Fig 1a.8 showed that goodness of fit ( $R^2$ ) between raw RCM and Bias corrected RCM were 0.875 and 0.975 respectively for validation period (1996-2005). So, it indicated that the value of CV was not exactly corrected for the validation period.

The Fig 1a.9 and Fig 1a.10 showed the comparison of skewness coefficient ( $C_s$ ) of observed, raw and bias corrected daily maximum temperature for calibration and validation period respectively. For calibration period it was found negative for all months and for validation period it was found positive for March and September and for rest of months it was found negative.

The Fig 1a.11 and Fig 1a.12 showed the comparison of Kurtosis coefficient ( $C_k$ ) of observed, raw and bias corrected daily maximum temperature for calibration and validation period respectively. For calibration period it was found positive for January, November and December and for rest of months it was found as negative and for validation period it was found positive for June and for rest of months it was found as negative. It can be seen that the bias correction by adopting Gaussian distribution cannot correct the third and fourth moments.



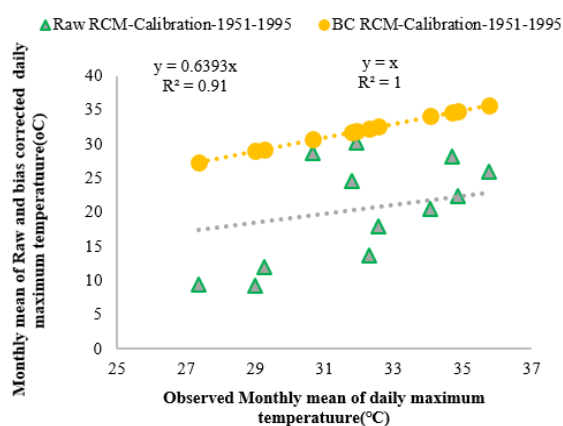


**Fig 1a.3: Comparison of the monthly mean of observed, raw and bias corrected daily maximum temperature during calibration period-1951-1995**

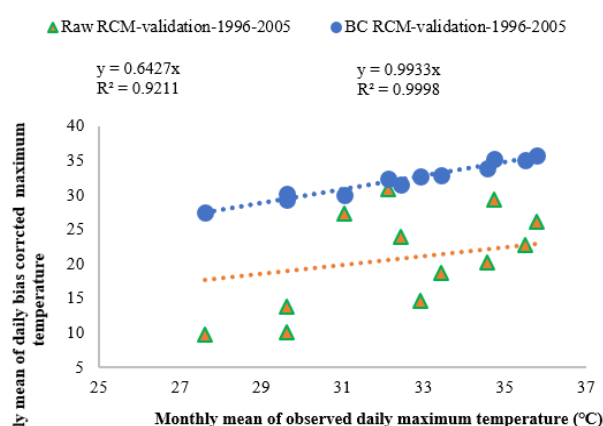


**Fig 1a.4: Comparison of the monthly mean of observed, raw and bias corrected daily maximum temperature during validation period-1996-2005**

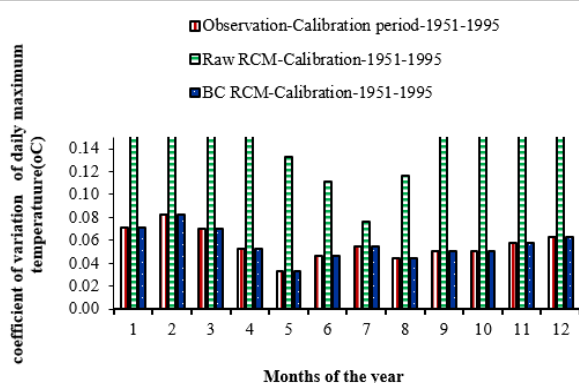


**Fig 1a.5: Comparison of the coefficient of variation of observed, raw and bias corrected daily maximum temperature during calibration period-1951-1995**

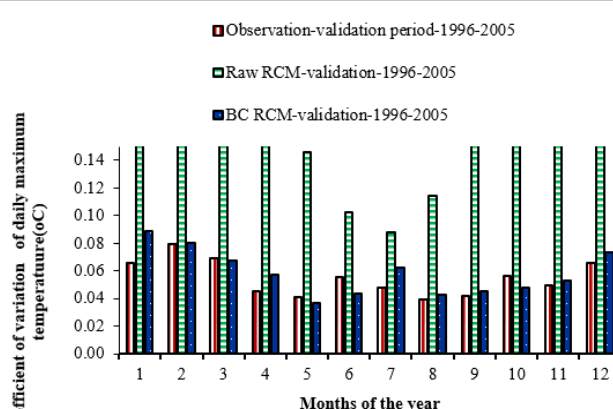


**Fig 1a.6: Comparison of the coefficient of variation of observed, raw and bias corrected daily maximum temperature during validation period-1996-2005**

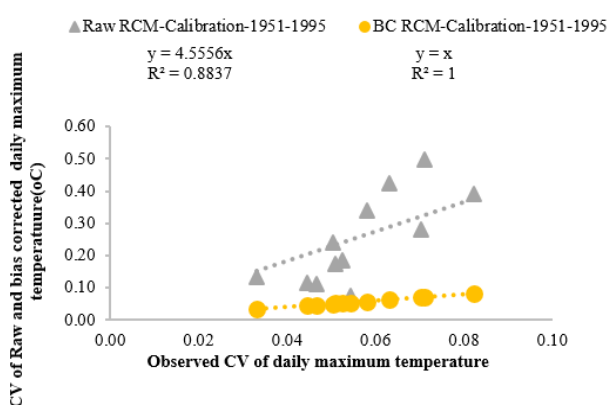


**Fig 1a.7: Comparison of the coefficient of variation of observed, raw and bias corrected daily maximum temperature during calibration period-1951-1995**

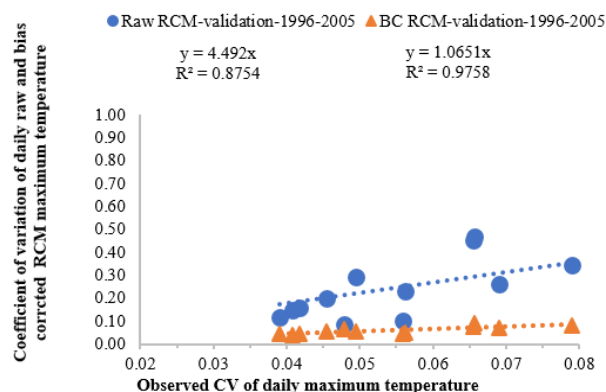


**Fig. 1a.8: Comparison of the coefficient of variation of observed maximum temperature during validation period-1996-2005)**

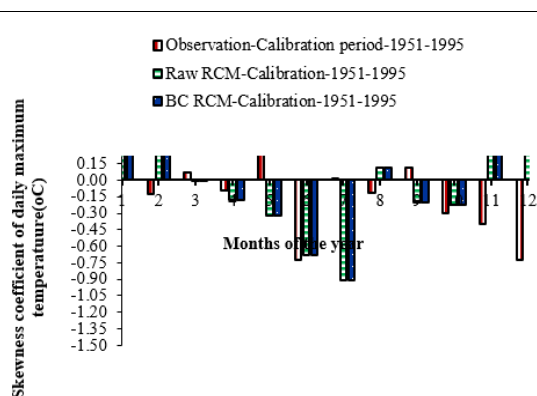


**Fig 1a.9: Comparison of the skewness coefficient of observed, raw and bias corrected daily maximum temperature during calibration period 1951-1995**

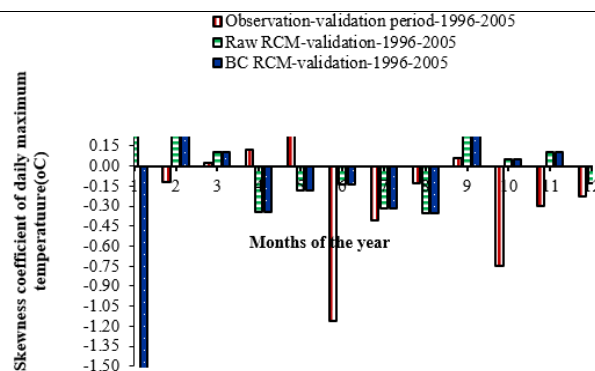


**Fig 1a.10: Comparison of the skewness coefficient of observed, raw and bias corrected daily maximum temperature during Validation period-1996-2005**

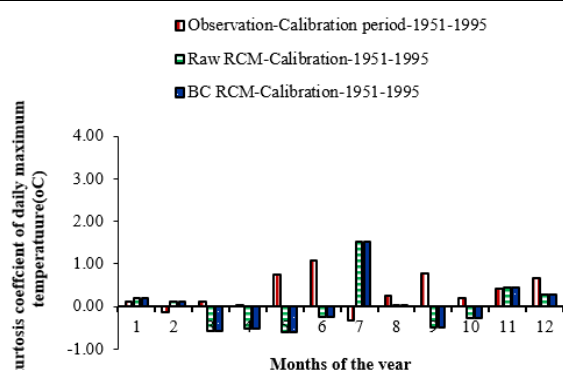


**Fig 1a.11: Comparison of the kurtosis coefficient of observed, raw and bias corrected daily maximum temperature during calibration period-1951-1995**

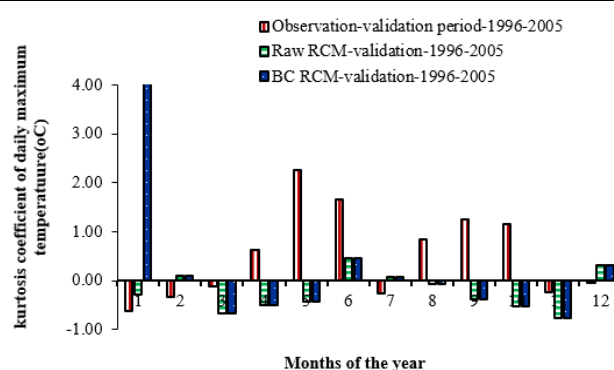


**Fig 1a.12: Comparison of the kurtosis coefficient of observed, raw and bias corrected daily maximum temperature during Validation period-1996-2005**

## B) Daily Minimum Temperature Control Scenario (1951-2005)

The computed monthly mean of daily observed, Raw RCM and Bias corrected RCM of minimum temperature of Rajkot for the calibration period (1951-1995) and validation period of (1996-2005) shown in Fig 1b.1 and Fig 1b.2. The considered statistics were the mean and coefficient of variation of the bias correction using the gaussian distribution mapping method. Fig 1b.1 showed that the raw RCM minimum temperature was underestimated over the observed monthly minimum temperature for all months for calibration period and Fig 1b.2 also showed the same result for the validation period. In fact, after applying the bias correction of Gaussian distribution method, the monthly mean for calibration period, (Fig 1b.1) and monthly mean for the validation period, (Fig 1b.2) of daily minimum temperature were agreed well with the actual observation during all of the 12 months of the year.

The relationship of monthly mean of observed minimum, Raw RCM and bias corrected RCM minimum temperature for calibration period (1951-1995) and validation period (1996-2005) were shown in Fig 1b.3 and Fig 1b.4. It could be seen from Fig 1b.3 that goodness of fit ( $R^2$ ) between raw RCM and Bias corrected RCM were 0.862 and 1 respectively for calibration period (1951-1995) and Fig 1b.4 shows that goodness of fit ( $R^2$ ) between raw RCM and Bias corrected RCM were 0.858 and 0.999 respectively for validation period (1996-2005), which showed that the gaussian distribution has corrected the first moment.

The coefficient of variation of observed, raw RCM and Bias corrected RCM daily minimum temperature of Rajkot during the

calibration and validation period was found as shown in Fig 1b.5 and Fig 1b.6. Fig 1b.5 Showed that the raw RCM daily maximum temperature with higher coefficient of variation than the observed minimum temperature data for all months. After applying the bias correction, the coefficient of variation of BC RCM minimum temperature were matched with the observed coefficient of variation of minimum temperature. For validation period (1996-2005), the coefficient of variation of both observed and bias corrected data were found lower than the coefficient of variation of raw RCM minimum temperature for all months. However, after applying the bias correction, the coefficient of variation of BC RCM minimum temperature were matched with the observed coefficient of variation of minimum temperature.

The relationship between the monthly coefficient of variation of observed, Raw and bias corrected daily minimum temperature for calibration period (1951-1995) and validation period (1996-2005) were shown in Fig 1b.7 and Fig 1b.8. It could be seen from Fig 1b.7 that goodness of fit ( $R^2$ ) between raw RCM and Bias corrected RCM were 0.5406 and 1 respectively for calibration period (1951-1995) which shows that data set was nearly matched with each other and Fig 1b.8 shows that goodness of fit ( $R^2$ ) between raw RCM and Bias corrected RCM were 0.503 and 0.991 respectively for validation period (1996-2005). So, it indicated that the value of CV was not exactly corrected for the validation period.

The Fig 1b.9 and Fig 1b.10 shows the comparison of skewness coefficient ( $C_s$ ) of observed, raw and bias corrected daily minimum temperature for calibration and validation period respectively. For calibration period it was found negative for all months except November and for validation period it was found

positive for November and for rest of months it was found negative.

The Fig 1b.11 and Fig 1b.12 shows the comparison of Kurtosis coefficient ( $C_k$ ) of observed, raw and bias corrected daily minimum temperature for calibration and validation period respectively. For calibration period it was found positive for

May, June, August and December and for rest of months it was negative and for validation period it was found positive for April, May and June and for rest of months it was found as negative. It can be seen that the bias correction by adopting Gaussian distribution cannot correct the third and fourth moments.

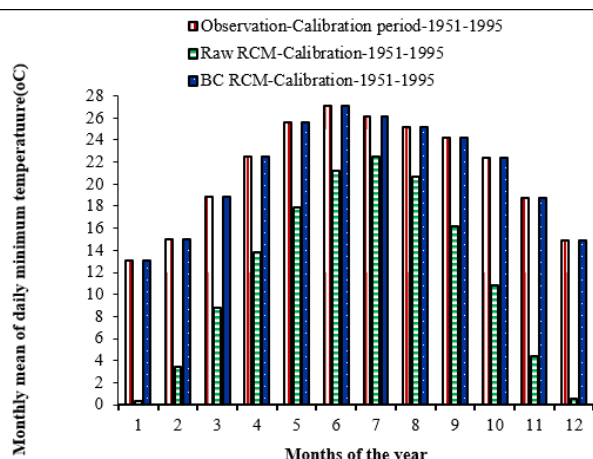


Fig 1b.1: Comparison of the monthly mean of observed, raw and bias corrected daily minimum temperature during calibration period-1951-1995

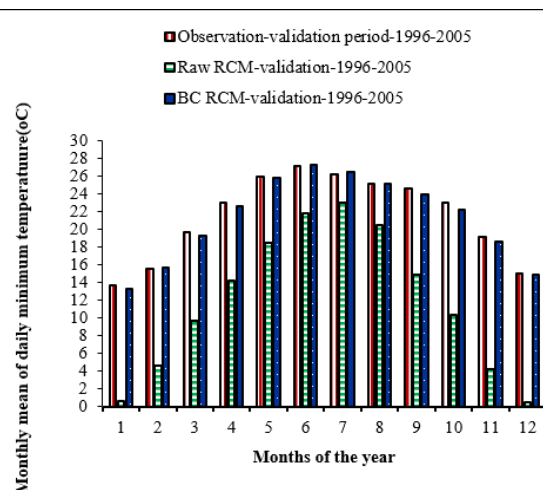


Fig 1b.2: Comparison of the monthly mean of observed, raw and bias corrected daily minimum temperature during validation period-1996-2005

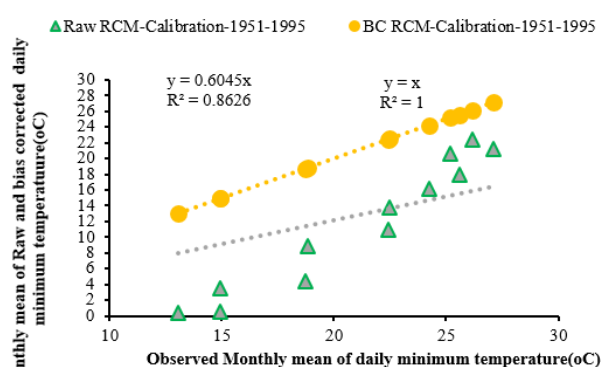


Fig 2b.3: Comparison of the monthly mean of observed, raw and bias corrected daily minimum temperature during calibration period-1951-1995

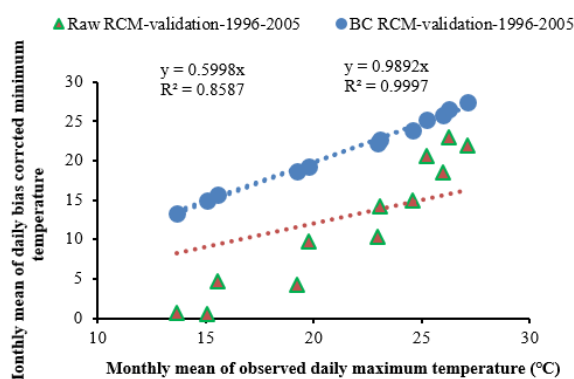


Fig 2b.4: Comparison of the monthly mean of observed, raw and bias corrected daily minimum temperature during validation period-1996-2005

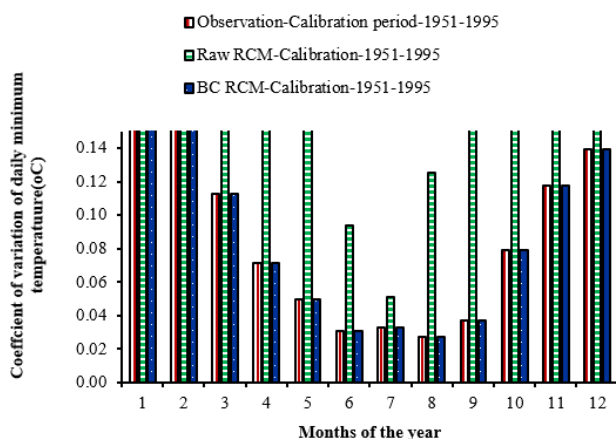


Fig 2b.5: Comparison of the coefficient of variation of observed, raw and bias corrected daily minimum temperature during calibration period-1951-1995

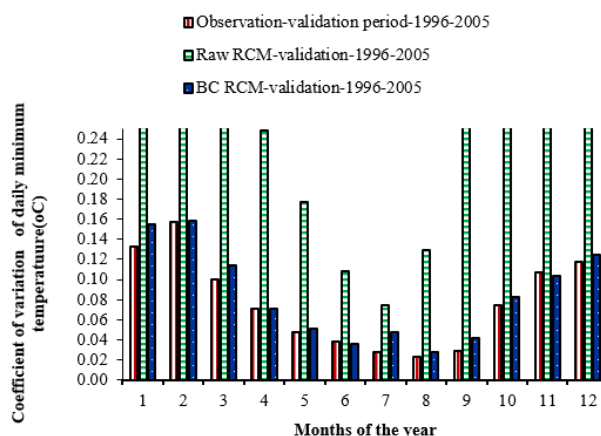
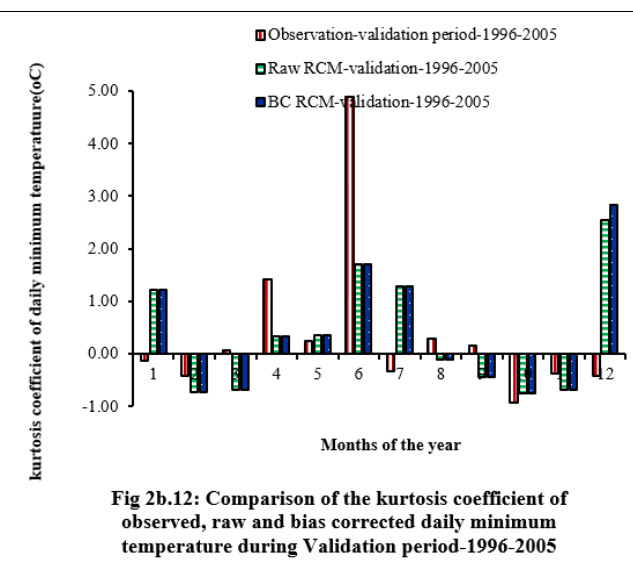
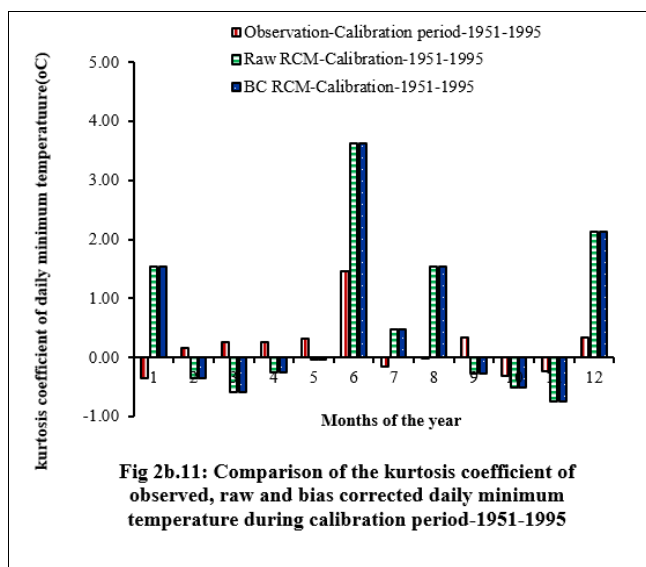
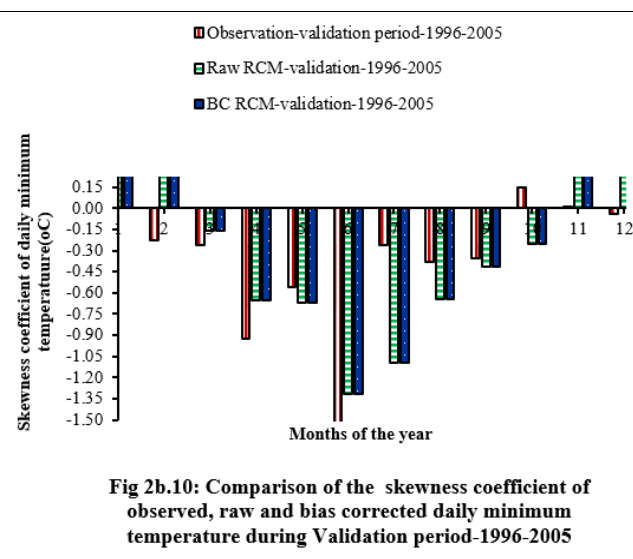
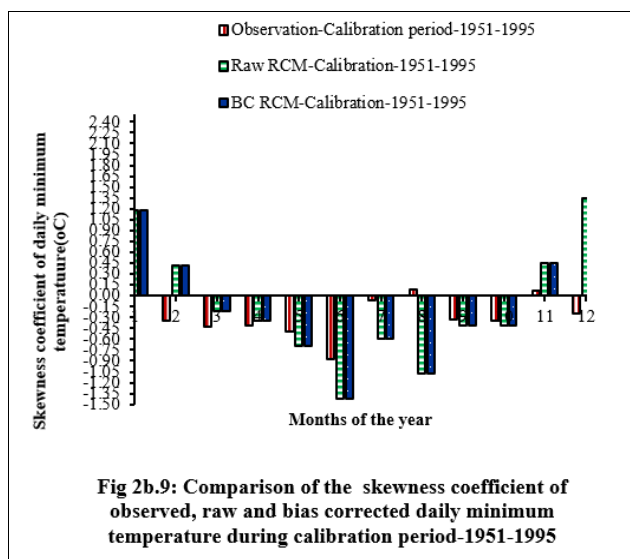
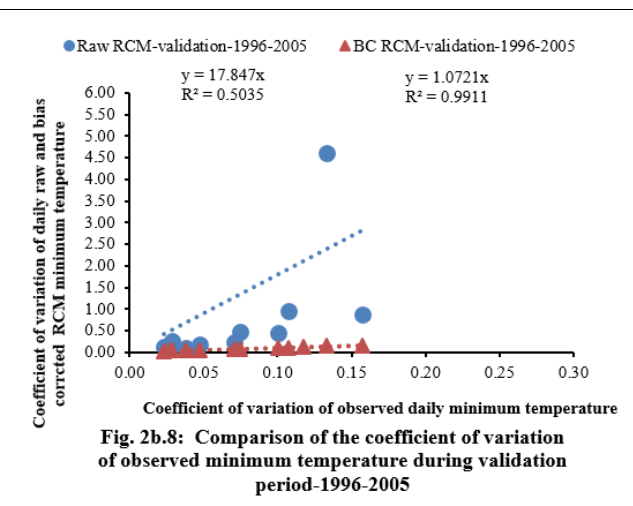
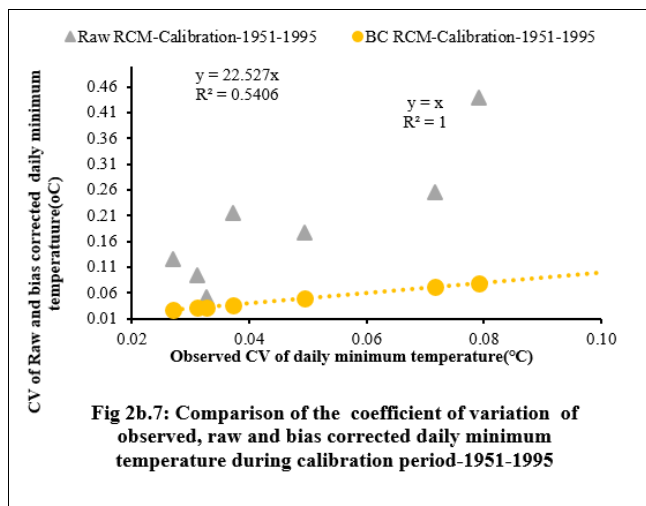


Fig 2b.6: Comparison of the coefficient of variation of observed, raw and bias corrected daily minimum temperature during validation period-1996-2005



## Future Period (2006-2100)

### RCP 2.6

#### A) Daily Maximum Temperature

Fig 3a.1, Fig 3a.2, Fig 3a.3 and Fig 3a.4 shows the statistical characteristics of raw and bias-corrected regional climate model (RCM) simulations from 2006 to 2100. Fig 3a.1 showed the mean temperatures, the mean temperature increased from January (29.10 °C) to May (37.17 °C), reaching a peak. This

suggested that May was likely the hottest month. After May, the mean temperature decreased, indicating the onset of the monsoon and post-monsoon cooling effects. There was a second peak in September (35.64 °C) and then temperatures gradually decrease towards December (31.65 °C).

Standard deviation indicates the amount of variation or dispersion from the mean. The SD was highest in March (2.78 °C) and lowest in September (1.26 °C). Months with higher SD



(March, April, June, and July) suggest greater variability in temperature, possibly due to transitional weather conditions or variable climate patterns. Lower SD in months like September indicated more stable temperatures with less fluctuation.

Fig 3a.2 showed the coefficient of variation ( $C_v$ ).  $C_v$  is the ratio of the standard deviation to the mean, expressed as a percentage. It provides a normalized measure of dispersion.  $C_v$  values ranged from 0.04 to 0.08, indicating relatively low variability in temperature across all months. This low variability suggested that while there are some fluctuations, temperatures remain relatively consistent around their mean.

Fig 3a.3 examined skewness coefficient ( $C_s$ ). Skewness measures the asymmetry of the data distribution around its mean.  $C_s$  values close to zero indicate a near-normal distribution. Positive skewness (e.g., January: 0.33, December: 0.35) implied a distribution with a longer tail on the right, meaning there are more instances of above-average temperatures. Negative skewness (e.g., April: -0.09, August: -0.08) suggested a longer left tail, with more occurrences of below-average temperatures. The majority of months have  $C_s$  values close to zero, indicating a roughly symmetrical distribution of temperature around the mean.

Fig 3a.4 shows Kurtosis coefficient ( $C_k$ ). Kurtosis measures the "tailedness" of the data distribution. A positive kurtosis (e.g., July: 0.43, August: 0.42) indicated a distribution with heavier tails and a sharper peak than a normal distribution, implying more extreme values. Negative kurtosis (e.g., February: -0.29, March: -0.40) suggested a flatter distribution with lighter tails, meaning fewer extreme temperature values. Most months have  $C_k$  values close to zero, indicating that the temperature distribution does not deviate significantly from a normal distribution.

## B) Daily Minimum Temperature

Fig 3b.1, Fig 3b.2, Fig 3b.3 and Fig 3b.4 showed the statistical characteristics of raw and bias-corrected regional climate model (RCM) simulations from 2006 to 2100. Fig 3b.1 showed the mean temperature, increasing from January (13.78 °C) to June (27.71 °C), indicating warming during the pre-monsoon period and reaching a peak in June and July. Post-July, the temperatures started to decrease gradually, reaching a low again in December (16.20 °C). This pattern aligned with typical

seasonal variations in the region, where temperature rise during the pre-monsoon season and drop during the winter months.

The SD was highest in March (2.69 °C) and lowest in August (0.54 °C). High SD values in the cooler months (e.g., January to March and November to December) suggested higher temperature variability, possibly due to the transition between winter and summer or between summer and monsoon seasons. Lower SD in monsoon and post-monsoon months (e.g., August) indicated more stable temperatures with less fluctuation, possibly due to the moderating effects of monsoon rains.

Fig 3b.2 showed the coefficients of variation ( $C_v$ ).  $C_v$  values range from 0.02 (August) to 0.17 (February), indicating varying degrees of relative temperature variability across the months. Higher  $C_v$  in the cooler months (January, February, November, December) suggested relatively higher variability compared to their means, while lower  $C_v$  in the warmer months (June, July, August) indicated more consistent temperatures relative to their means.

Fig 3b.3 showed the skewness coefficient ( $C_s$ ). Positive skewness (e.g., January: 1.31, February: 0.55, December: 1.17) indicated that the temperature distributions were right-skewed with more instances of below-average temperatures and occasional higher extreme temperatures. Negative skewness (e.g., April: -0.22, July: -0.40, August: -1.16) suggested a left-skewed distribution with more occurrences of above-average temperatures and some lower extreme temperatures. Months with near-zero skewness (e.g., March: -0.02, October: -0.05) have temperature distributions that were approximately symmetric around the mean.

Fig 3b.4 shows the Kurtosis coefficient ( $C_k$ ). Positive kurtosis (e.g., January: 1.28, July: 1.98, August: 1.82) indicated a distribution with heavier tails and a sharper peak than a normal distribution, implying a higher likelihood of extreme temperature values (either hot or cold). Negative kurtosis (e.g., February: -0.53, March: -0.41, October: -0.66) suggested a flatter distribution with lighter tails, meaning fewer extreme temperature values. The presence of both positive and negative kurtosis across different months indicated that temperature distributions could be quite varied, with some months experiencing more extreme temperature variability and others more moderate, stable conditions.

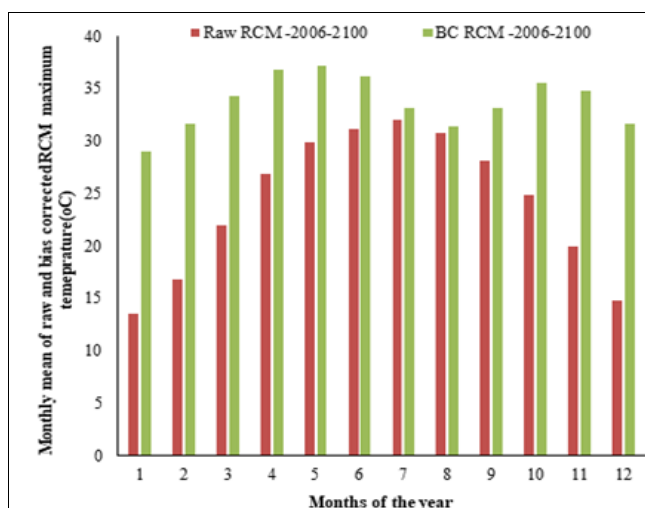


Fig. 3a.1 Comparison of raw and bias corrected RCM monthly mean of daily maximum temperature during future scenario-2006-2100

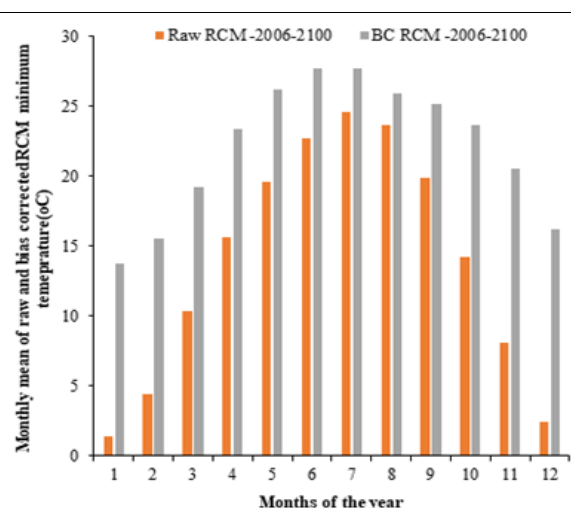


Fig. 3b.1 Comparison of raw and bias corrected RCM monthly mean of daily minimum temperature during future period-2006-2100

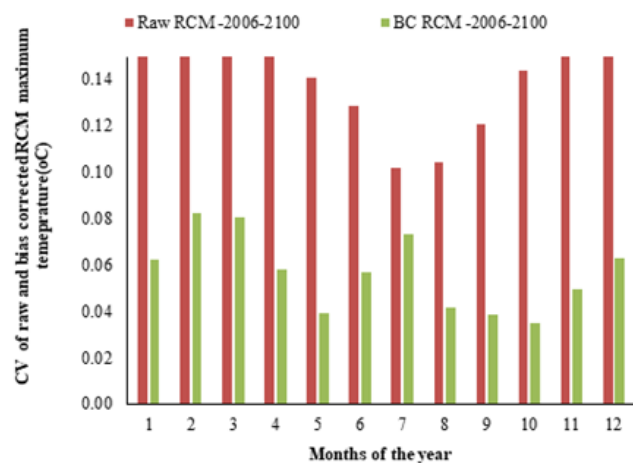


Fig. 3a.2 Comparison of CV of raw and bias corrected RCM daily maximum temperature during future period-2006-2100

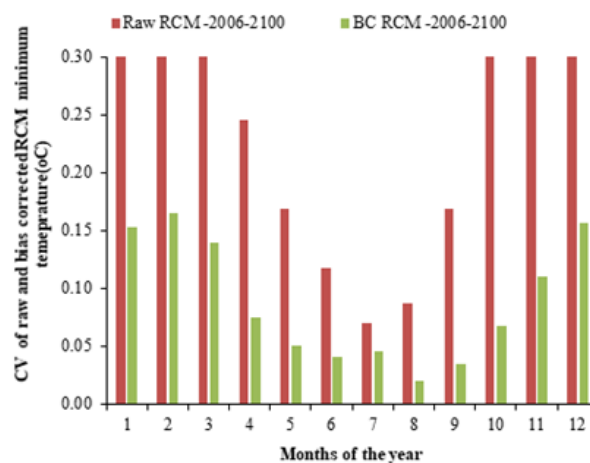


Fig. 3b.2 Comparison of CV of raw and bias corrected RCM daily minimum temperature during future period-2006-2100

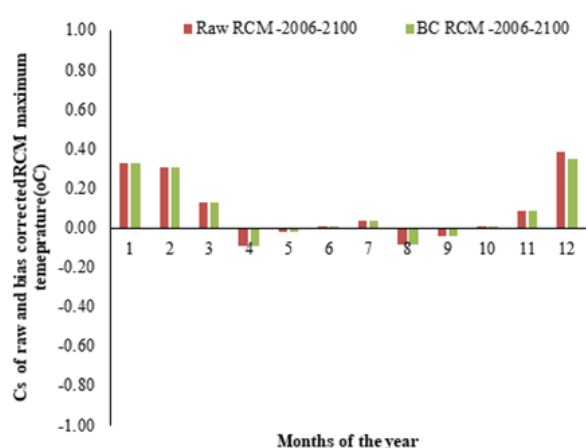


Fig. 3a.3 Comparison of Cs of raw and bias corrected RCM daily maximum temperature during future period-2006-2100

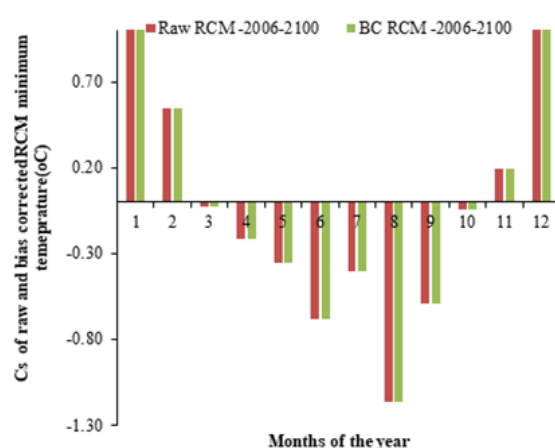


Fig. 3b.3 Comparison of Cs of raw and bias corrected RCM daily minimum temperature during future period-2006-2100

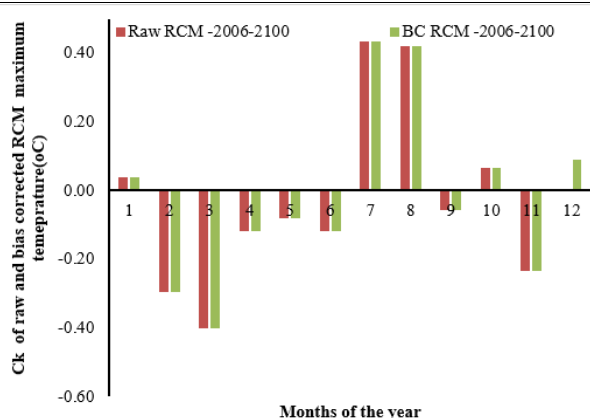


Fig. 3a.4 Comparison of Ck of raw and bias corrected RCM daily maximum temperature during future period-2006-2100

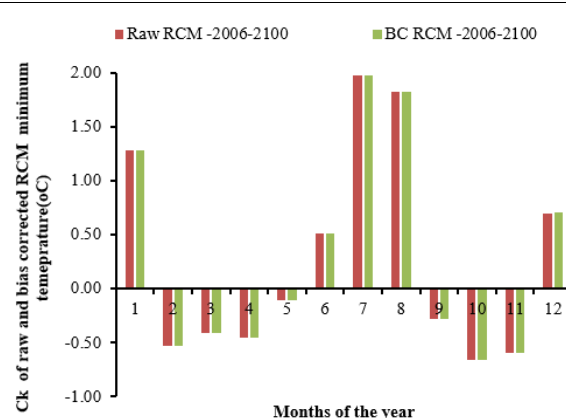


Fig. 3b.4 Comparison of Ck of raw and bias corrected RCM daily minimum temperature during future period-2006-2100

## Future Period (2006-2100)

### RCP 4.5

#### A) Daily Maximum Temperature

Fig 4a.1, Fig 4a.2, Fig 4a.3 and Fig 4a.4 showed the statistical characteristics of raw and bias-corrected regional climate model

(RCM) simulations for the period 2006-2100. Fig 4a.1 showed the mean daily maximum temperatures, the mean temperatures increase steadily from January (28.66°C) to May (36.44°C), indicating a warming trend leading up to the pre-monsoon period. June (36.14°C) marked a slight decrease, indicating the

start of the monsoon season which typically moderates temperature. After June, temperature gradually declined through to December (30.76°C), following a post-monsoon cooling and the onset of winter.

Standard deviation measured the variability or dispersion of temperature values around the mean. SD values ranged from a minimum of 1.17°C in May to a maximum of 2.58°C in July. Higher SD values in months like February (2.40°C), March (2.47°C), and July (2.58°C) indicated more significant temperature variability during these periods. Lower SD values in May (1.17°C) and August (1.42°C) suggested more stable temperatures during these months, likely due to more consistent climatic conditions.

Fig 4a.2 showed coefficient of variation (Cv). Cv values range from 0.03 (May) to 0.08 (February), indicating relatively low variability across all months. Months with higher Cv, like February (0.08) and March (0.07), have slightly more relative variability compared to their mean, which could be due to transitional weather conditions. Lower Cv values, particularly in May (0.03), indicate consistent temperature with less relative fluctuation around the mean.

Fig 4a.3 showed the Skewness coefficient (Cs). Positive skewness values (e.g., January: 0.42, February: 0.44, March: 0.22) indicated that these months have more instances of below-average temperatures with occasional higher extreme temperatures, resulting in a right-skewed distribution. Negative skewness values (e.g., April: -0.24, May: -0.54, August: -0.43) suggested a left-skewed distribution with more occurrences of above-average temperatures and fewer extreme low temperatures. The skewness values close to zero (e.g., June: -0.10, October: -0.12) indicate that temperature distributions were approximately symmetric around the mean.

Fig 4a.4 showed the Kurtosis coefficient (C<sub>K</sub>). Positive kurtosis values (e.g., January: 0.58, June: 1.45, December: 0.93) indicated a distribution with heavier tails and a sharper peak than a normal distribution, suggesting a higher likelihood of extreme values (either hot or cold). Negative kurtosis values (e.g., March: -0.34, April: -0.27) suggested a flatter distribution with lighter tails, meaning fewer extreme temperature values. Months with kurtosis values close to zero (e.g., October: -0.01, November: -0.03) have a distribution that does not deviate significantly from a normal distribution, indicating a balance in the frequency of extreme and average temperatures.

## B) Daily Maximum Temperature

Fig 4b.1, Fig 4b.2, Fig 4b.3 and Fig 4b.4 showed the statistical characteristics of raw and bias-corrected regional climate model

(RCM) simulations for the period 2006-2100. Fig 4b.1 showed the mean daily minimum temperatures, the mean temperatures increase from January (13.35°C) to June (27.81°C), indicating a warming trend leading up to the pre-monsoon period. After June, temperature slightly decrease, reaching a minimum in December (16.24°C). This pattern reflected the typical seasonal cycle, with the warmest months occurring just before the monsoon and cooler temperature following the monsoon and continuing through winter.

SD values range from a minimum of 0.44°C in August to a maximum of 2.56°C in December. Higher SD values in the cooler months (January, February, November, December) suggested more significant temperature variability, which could be due to greater fluctuation between daytime and nighttime temperatures or weather transitions in those months. Lower SD values in June (0.84°C) and August (0.44°C) indicated more stable temperatures, likely due to consistent monsoon conditions and cloud cover moderating temperatures.

Fig 4b.2 showed coefficient of variation (Cv). Cv values range from 0.02 (August) to 0.16 (February and December), indicating that relative variability is higher in the cooler months and lower during the monsoon months. The highest Cv values in February (0.16) and December (0.16) suggest higher relative temperature variability during these months, possibly due to the transition between seasons or fluctuating weather patterns.

Fig 4b.3 showed the Skewness coefficient (Cs). Positive skewness values (e.g., January: 1.67, February: 0.54, December: 1.04) indicate a right-skewed distribution, with more instances of below-average temperatures and occasional extreme high temperatures. Negative skewness values (e.g., April: -0.28, May: -0.85, June: -1.04, September: -1.03) indicated a left-skewed distribution, with more instances of above-average temperatures and occasional extreme low temperatures. Skewness values near zero (e.g., March: 0.06, November: 0.03) suggest a roughly symmetrical distribution of temperatures around the mean.

Fig 4b.4 showed the Kurtosis coefficient (C<sub>K</sub>). Positive kurtosis values (e.g., January: 2.97, June: 3.44, September: 0.97) indicated distributions with heavier tails and sharper peaks than a normal distribution, suggesting a higher likelihood of extreme values (either hot or cold). Negative kurtosis values (e.g., February: -0.44, March: -0.37, October: -0.26, November: -0.70) suggested flatter distributions with lighter tails, meaning fewer extreme temperature values. The range of kurtosis values showed that while some months have a distribution that deviate significantly from a normal distribution, others were closer to a normal distribution.

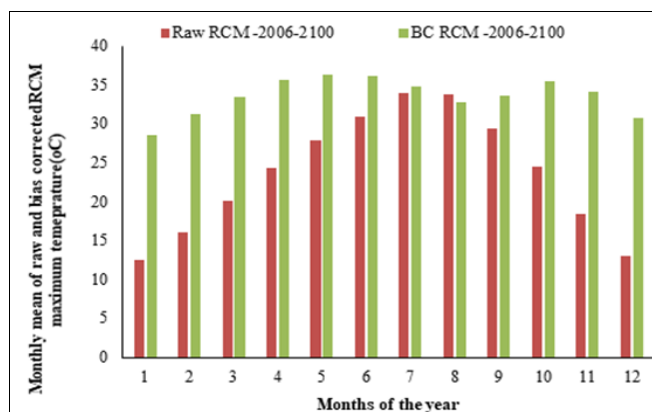


Fig. 4a.1 Comparison of raw and bias corrected RCM monthly mean of daily maximum temperature during future scenario-2006-2100

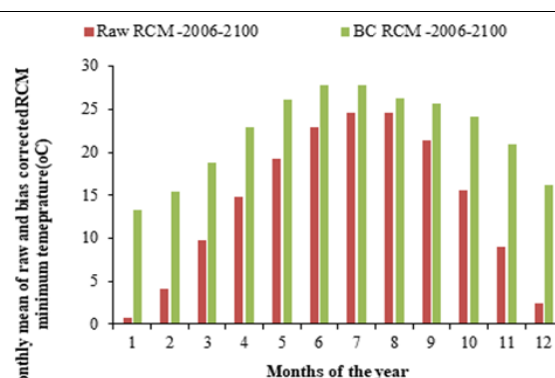


Fig. 4b.1 Comparison of raw and bias corrected RCM monthly mean of daily minimum temperature during future period-2006-2100

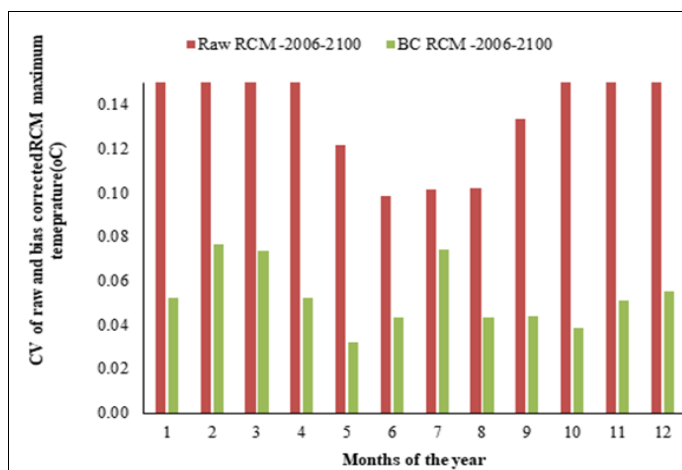


Fig. 4a.2 Comparison of CV of raw and bias corrected RCM daily maximum temperature during future period-2006-2100

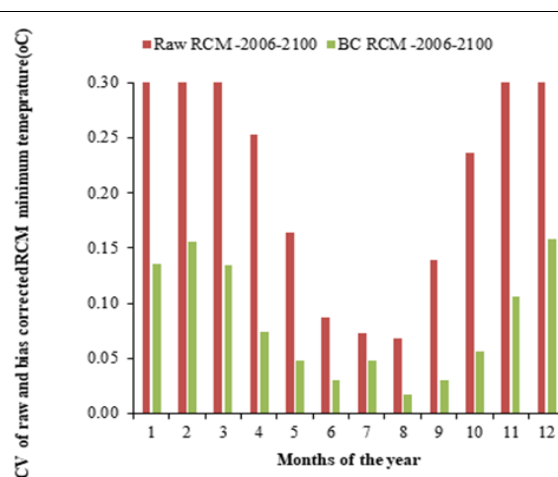


Fig. 4b.2 Comparison of CV of raw and bias corrected RCM daily minimum temperature during future period-2006-2100

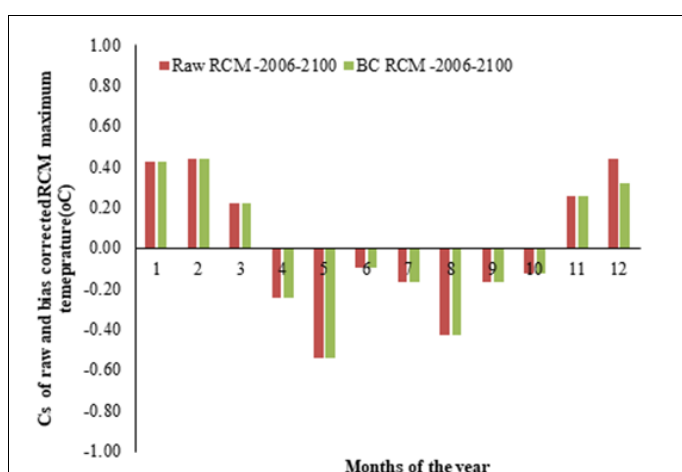


Fig. 4a.3 Comparison of Cs of raw and bias corrected RCM daily maximum temperature during future period-2006-2100

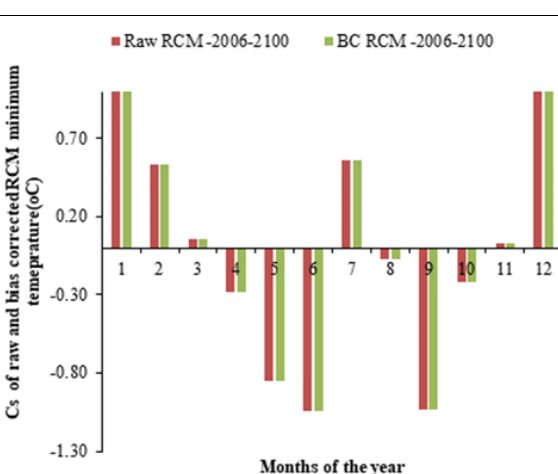


Fig. 4b.3 Comparison of Cs of raw and bias corrected RCM daily minimum temperature during future period-2006-2100

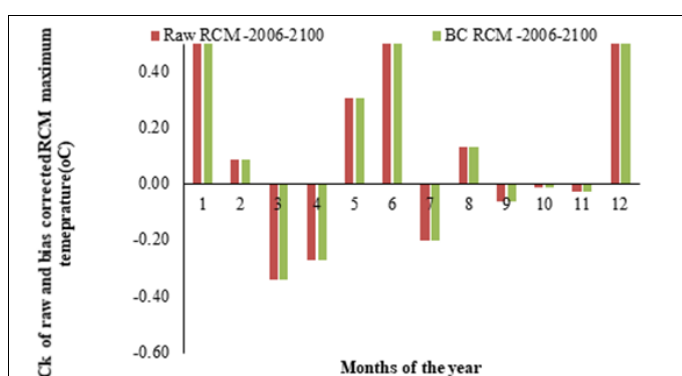


Fig. 4a.4 Comparison of Ck of raw and bias corrected RCM daily maximum temperature during future period-2006-2100

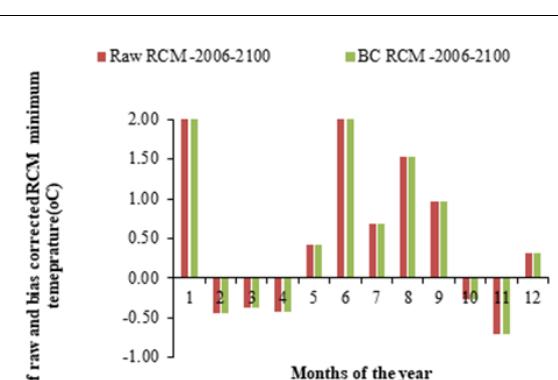


Fig. 4b.4 Comparison of Ck of raw and bias corrected RCM daily minimum temperature during future period-2006-2100

## Future Period (2006-2100)

### RCP 8.5

#### A) Daily Maximum Temperature

Fig 5a.1, Fig 5a.2, Fig 5a.3 and Fig 5a.4 showed the statistical characteristics of raw and bias-corrected regional climate model (RCM) simulations for the period 2006-2100. Fig 5a.1 shows the

mean daily maximum temperatures, the mean temperatures show a gradual increase from January ( $30.51^{\circ}\text{C}$ ) to May ( $38.67^{\circ}\text{C}$ ), indicating a warming trend leading up to the hottest part of the year. June ( $37.91^{\circ}\text{C}$ ) shows a slight decrease from May, reflecting the onset of the monsoon season. From July onwards, temperatures decrease, reaching their lowest in



December (31.52°C), following the typical seasonal cooling pattern after the monsoon and into winter. SD values range from a minimum of 1.44°C in August to a maximum of 2.91°C in February. Higher SD values in months like February (2.91°C) and March (2.59°C) suggest greater temperature variability during these months, likely due to transitional weather conditions. Lower SD values in August (1.44°C) and May (1.56°C) suggest more stable temperatures, likely due to consistent climatic conditions during the monsoon and the beginning of summer.

Fig 5a.2 shows Coefficient of Variation (Cv). Cv values range from 0.04 (May, August, September, October) to 0.09 (February), indicating relatively low variability across all months. February, with the highest Cv value (0.09), indicates more relative variability compared to its mean, which could be due to winter weather variability. Months like May, August, and September, with lower Cv values (0.04), indicate consistent temperatures with less relative fluctuation around the mean.

Fig 5a.3 shows the skewness coefficient. Positive skewness values (e.g., January: 0.43, February: 0.41, May: 0.25) indicate that these months have more instances of below-average temperatures with occasional higher extreme temperatures, resulting in a right-skewed distribution. Negative skewness values (e.g., July: -0.14, October: -0.15, December: -0.06) suggest a left-skewed distribution with more occurrences of above-average temperatures and fewer extreme low temperatures. The skewness values close to zero (e.g., March: 0.01, April: 0.01, November: 0.02) indicate that temperature distributions are approximately symmetric around the mean.

Fig 5a.4 shows the kurtosis coefficient. Positive kurtosis values (e.g., January: 0.16, June: 0.62, December: 1.11) indicate a distribution with heavier tails and a sharper peak than a normal distribution, suggesting a higher likelihood of extreme values (either hot or cold). Negative kurtosis values (e.g., February: -0.13, March: -0.61, April: 0.00) suggest a flatter distribution with lighter tails, meaning fewer extreme temperature values. Months with kurtosis values close to zero (e.g., April: 0.00, October: 0.06) have a distribution that does not deviate significantly from a normal distribution, indicating a balance in the frequency of extreme and average temperatures.

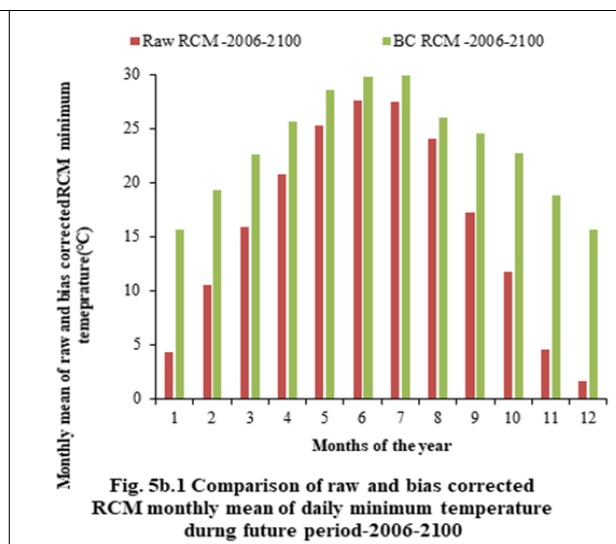
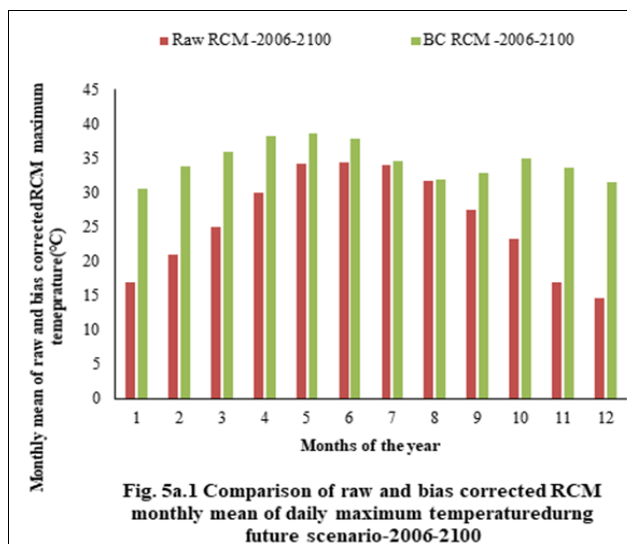
## B) Daily Minimum Temperature

Fig 5b.1, Fig 5b.2, Fig 5b.3 and Fig 5b.4 showed the statistical characteristics of raw and bias-corrected regional climate model (RCM) simulations for the period 2006-2100. Fig 5b.1 showed

the mean daily minimum temperatures, the mean temperatures showed an increase from January (15.70°C) to July (29.85°C), indicating a warming trend towards the middle of the year, which was typical for this region as it moves towards the summer. The highest mean temperature was in July (29.85°C), after which there was a gradual decrease until December (15.70°C), reflecting the cooling trend into the winter season. SD values range from a minimum of 0.85°C in August to a maximum of 3.22°C in February. The higher SD values in January (2.99°C) and February (3.22°C) suggested greater temperature variability during these winter months, which could be due to more unpredictable weather patterns. Lower SD values in August (0.85°C) and July (0.92°C) suggested more stable temperatures during the peak summer and early monsoon period. Fig 5b.2 showed the coefficient of variation. Cv values range from 0.03 (July and August) to 0.19 (January), indicating low relative variability in summer months and higher relative variability in winter months. The highest Cv in January (0.19) indicated a higher relative variability in temperatures, which can be associated with colder months that often have more fluctuations in daily temperatures. Lower Cv value in July and August (0.03) indicated more consistent temperatures relative to their means during these stable, warm months.

Fig 5b.3 showed the skewness coefficient. Positive skewness values (e.g., January: 0.66, November: 0.64, December: 1.43) indicated that these months have more instances of below-average temperatures with occasional higher extreme temperatures, resulting in a right-skewed distribution. Negative skewness values (e.g., March: -0.17, April: -0.24, August: -0.55) suggested a left-skewed distribution, indicating more occurrences of above-average temperatures with fewer lower extremes. Months with skewness values close to zero (e.g., October: 0.02, September: -0.02) have temperature distributions that are approximately symmetric around the mean.

Fig 5b.4 showed kurtosis coefficient. Positive kurtosis values (e.g., July: 0.61, December: 2.17) indicated a distribution with heavier tails and a sharper peak than a normal distribution, suggested a higher likelihood of extreme values (either hot or cold). Negative kurtosis values (e.g., January: -0.25, February: -0.32, March: -0.48) suggested a flatter distribution with lighter tails, meaning fewer extreme temperature values. Months with kurtosis values close to zero (e.g., April: -0.15, May: 0.01) have a distribution that does not deviate significantly from a normal distribution, indicating a balance in the frequency of extreme and average temperatures.



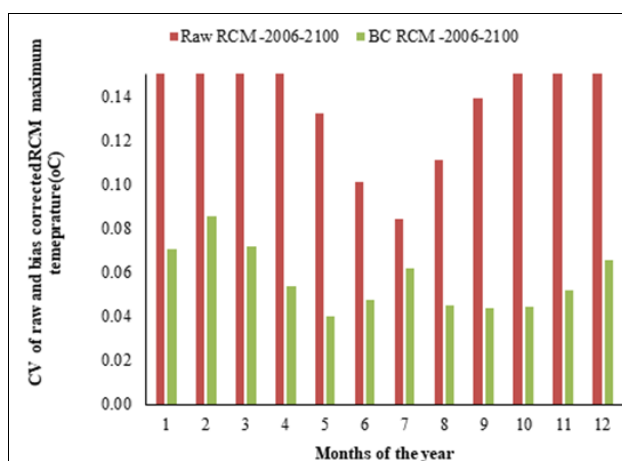


Fig. 5a.2 Comparison of CV of raw and bias corrected RCM daily maximum temperature during future period-2006-2100

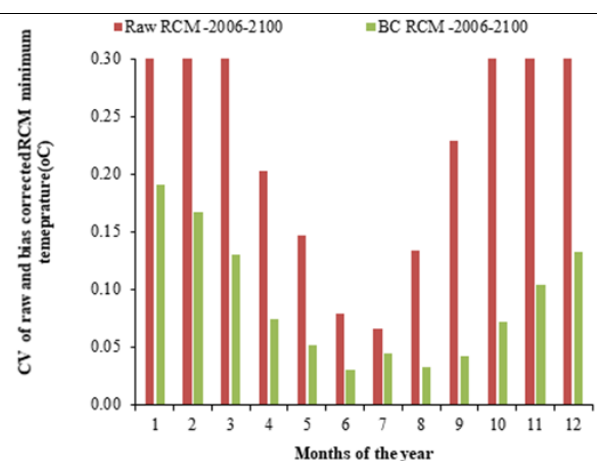


Fig. 5b.2 Comparison of CV of raw and bias corrected RCM daily minimum temperature during future period-2006-2100

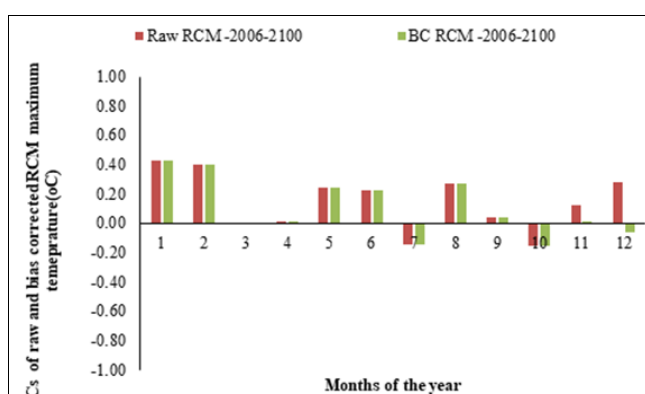


Fig. 5a.3 Comparison of Cs of raw and bias corrected RCM daily maximum temperature during future period-2006-2100

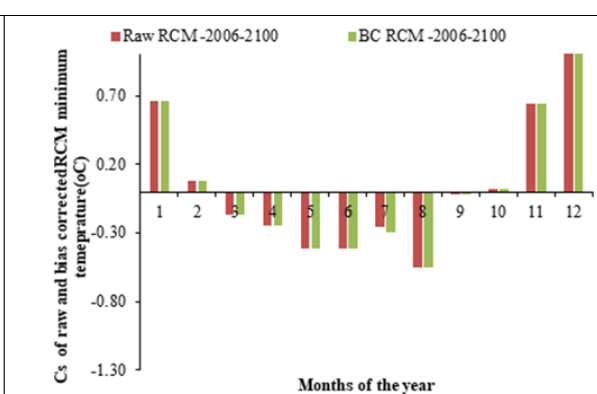


Fig. 5b.3 Comparison of Cs of raw and bias corrected RCM daily minimum temperature during future period-2006-2100

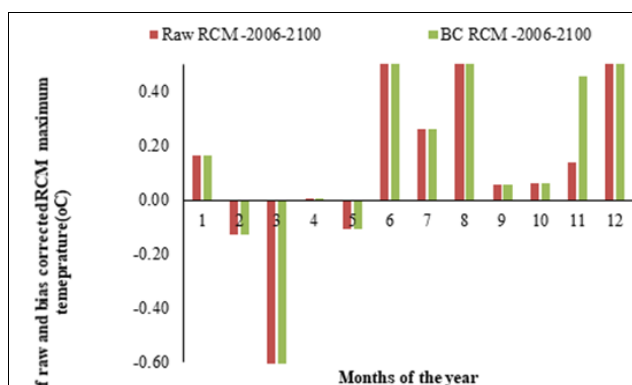


Fig. 5a.4 Comparison of Ck of raw and bias corrected RCM daily maximum temperature during future period-2006-2100

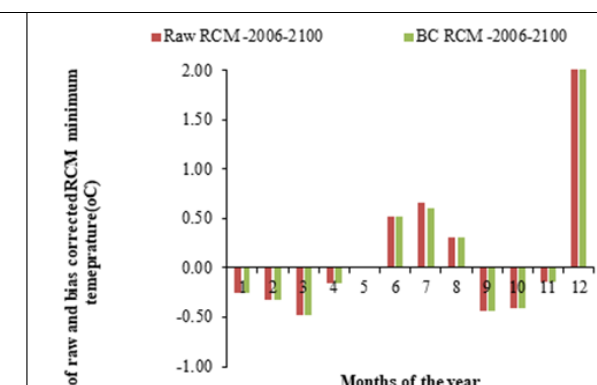


Fig. 5b.4 Comparison of Ck of raw and bias corrected RCM daily minimum temperature during future period-2006-2100

## Conclusion

The study shows a comprehensive bias correction analysis on daily maximum and minimum temperatures for Rajkot, focusing on the baseline period (1951-2005) and future scenarios (2006-2100) under three Representative Concentration Pathways (RCP 2.6, RCP 4.5, and RCP 8.5). The bias correction process used the Gaussian distribution mapping method to adjust the simulated data from the RCA4 regional climate model (RCM) against observed data, ensuring a more accurate representation

of temperature trends.

For daily maximum temperatures during the control period (1951-2005), the raw RCM data consistently underestimated observed temperatures across all months during both the calibration (1951-1995) and validation (1996-2005) phases. The Gaussian distribution mapping method significantly corrected these biases, bringing the bias-corrected RCM data in close agreement with observed data for all months. This was confirmed by high  $R^2$  values, indicating a strong goodness of fit

between the bias-corrected and observed data. The coefficient of variation (CV) for the bias-corrected data also closely matched the observed data, demonstrating that the method effectively adjusted for variability. However, the bias correction method was less effective in fully correcting the skewness (third moment) and kurtosis (fourth moment), suggesting limitations in adjusting the tails and peaks of the temperature distribution.

For daily minimum temperatures during the same period, a similar pattern was observed. The raw RCM data underestimated observed minimum temperatures, but after applying the Gaussian distribution mapping method, the bias-corrected data closely aligned with the observed data in terms of mean temperatures and CVs. Yet, like with maximum temperatures, there were notable discrepancies in skewness and kurtosis between the bias-corrected and observed data, indicating that while the correction method effectively adjusted for mean temperature biases, it did not fully account for the distribution's shape.

In future scenarios (2006-2100), the analysis under RCP 2.6, RCP 4.5, and RCP 8.5 highlighted distinct temperature trends. Under RCP 2.6 and RCP 4.5, there was a noticeable warming trend before the monsoon season and cooling post-monsoon. The bias correction process-maintained consistency in these projections, ensuring that mean temperatures were aligned with expected trends. However, under the more extreme RCP 8.5 scenario, the warming trends were more pronounced across all months, reflecting a significant increase in maximum and minimum temperatures due to higher greenhouse gas concentrations.

Despite the effectiveness of the bias correction in aligning simulated data with observed mean temperatures across all RCP scenarios, variations in standard deviation, skewness, and kurtosis across different months indicated persistent challenges in accurately modeling temperature extremes and variability. These variations suggest that while the Gaussian distribution mapping method is robust for correcting mean biases, it has limitations in adjusting higher-order statistical moments, which are crucial for understanding the full range of temperature variability and extreme events in the future.

## References

1. Casanueva A, Herrera S, Iturbide M, Lange S, Jury M, Dosio A. Testing bias adjustment methods for regional climate change applications under observational uncertainty and resolution mismatch. *Atmospheric Science Letters*. 2020;21(4):e978.
2. Chen J, Brissette FP, Chaumont D, Braun M. Finding appropriate bias correction methods in downscaling precipitation for hydrologic impact studies over North America. *Water Resources Research*. 2013;49(7):4187-4205.
3. Eccles R, Zhang H, Hamilton D, Trancoso R, Syktus J. Impacts of climate change on streamflow and floodplain inundation in a coastal subtropical catchment. *Advances in Water Resources*. 2021;147:103-115.
4. Ehret U, Zehe E, Wulfmeyer V, Warrach-Sagi K, Liebert J. Should we apply bias correction to global and regional climate model data? *Hydrology and Earth System Sciences*. 2012;16(9):3391-3404.
5. Frei C, Schöll R, Fukutome S, Schmidli J, Vidale PL. Future change of precipitation extremes in Europe: Intercomparison of scenarios from regional climate models. *Journal of Geophysical Research Atmospheres*. 2006;111:D06105.
6. Grose MR, Syktus J, Thatcher M, Evans JP, Ji F, Rafter T. The role of topography on projected rainfall changes in mid-latitude mountain regions. *Climate Dynamics*. 2019;53(6-7):3675-3690.
7. Maraun D. Bias correcting climate change simulations - A critical review. *Current Climate Change Reports*. 2016;2(4):211-220.
8. Teutschbein C, Seibert J. Bias correction of regional climate model simulations for hydrological climate-change impact studies: Review and evaluation of different methods. *Journal of Hydrology*. 2012;456:12-29.
9. Trancoso R, Syktus J, Toombs N, Ahrens D, Wong KKH, Pozza RD. Heatwaves intensification in Australia: A consistent trajectory across past, present and future. *Science of the Total Environment*. 2020;742:140-152.